Lightning Efficient Counterpoise Configurations for Transmission Line Grounding

Leonid Grcev, *Life Fellow, IEEE*, Blagoja Markovski, and Mirko Todorovski, *Senior Member, IEEE*

***Abstract*—Different configurations of counterpoises are often used to reduce the resistance and impulse impedance of the transmission line grounding. However, there are no general rules for an actual design. This paper analyses the performance of several configurations of counterpoises under typical lightning current impulses. The basis is a parametric analysis derived from time responses of 11,386 test cases for each configuration with parameters in broad ranges computed using a rigorous electromagnetic model based on the method of moments. The contributions of the paper are: Simple formulas for the resistance, impulse impedance, and effective length of counterpoise configurations are derived from and verified by the simulation results; a configuration with an 8-leg counterpoise bent parallel to the line is proposed, which extends the effective length and is efficient in high resistivity soil; and the method does not depend on the different lightning current impulse waveform representations based on Heidler, CIGRE, and double-exponential formulas, since the results can be easily converted. A simple procedure is provided to compare the capabilities and limitations of counterpoise configurations. New formulas and procedures make up a general and straightforward method for analyzing the optimal design, considering the cost-effective and best protection against lightning.**

***Index Terms*—Transmission lines, lightning protection, grounding, modeling.**

I. Introduction

THE reliability of power systems depends on the lightning performance of transmission lines. Such performance is improved by reducing the transmission line grounding resistance R and impulse impedance Z [1], [2], [3]. The most effective way of lowering R, especially in medium-to-high resistive soil, is by long horizontal grounding electrodes (known as "counterpoises"). However, there is a limit to reducing Z since it becomes constant for grounding larger than a limiting size called "effective."

Manuscript received 26 April 2022; revised 13 July 2022; accepted 15 August 2022. Date of publication 22 August 2022; date of current version 24 March 2023. This work was supported in part by the Ss. Cyril and Methodius University in Skopje under Project NIP.UKIM.20-21.10 and in part by the Macedonian Academy of Sciences and Arts. Paper no. TPWRD-00602-2022. *(Corresponding author: Leonid Grcev.)*

Leonid Grcev is with the Macedonian Academy of Sciences and Arts, Skopje 1000, Macedonia (e-mail: lgrcev@feit.ukim.edu.mk).

Blagoja Markovski and Mirko Todorovski are with the Faculty of Electrical Engineering and Information Technologies, Ss. Cyril and Methodius University in Skopje, Skopje 1000, Macedonia (e-mail: bmarkovski@feit.ukim.edu.mk; mirko@feit.ukim.edu.mk).

Color versions of one or more figures in this article are available at https://doi.org/10.1109/TPWRD.2022.3200579.

Digital Object Identifier 10.1109/TPWRD.2022.3200579

The problem of enlarging grounding's effective size is one of the recently researched topics and one of the most intricate, e.g., [4], [5], [6], [7], [8], [9], [10]. Recent standards and recommendations by IEEE, CIGRE, and EPRI have covered this topic [11], [12], [13], [14], [15], [16], but "there is no consensus yet on how to apply present knowledge to the design of the actual electrode system" [17].

This paper aims to develop a method for evaluating the optimal counterpoise configuration of overhead transmission line grounding for best protection against lightning. The method's basis is simple formulas that are derived and validated using simulation results of the time responses of 11386 test cases for each configuration with parameters in broad ranges. Simulations are performed using a rigorous electromagnetic model [18], [19], [20]. The model computes the grounding electrodes' current distribution by numerically solving the electric field integral equation in the frequency domain by the method of moments. The corresponding Green functions are based on a mathematically exact solution of the electromagnetic field in a layered medium, which involves Sommerfeld integrals. Such integrals cannot be solved analytically; however, accurate computations are today possible using dedicated computer software, e.g., [48]. The solution is not limited in frequency and includes all electromagnetic propagation effects. Required quantities, such as GPR, can be straightforwardly computed from known currents. Fourier transformation techniques are used to obtain the time-domain response to lightning currents. Olsen et al. [21] have established this model as an "exact" solution to this problem and a "gold standard" for comparisons. Since this model is compared with many experimental results, e.g., [22], [23], [24], [25], the simple formulas are consistent with these experiments. The original contributions of this paper are:

- A complete set of new formulas of resistance, impulse impedance, and effective length for analyzing the lightning efficiency of different counterpoise configurations is derived.
- A configuration with an 8-leg counterpoise is proposed, which, compared to the usual 4-leg configuration, enlarges the effective length and is more efficient in high resistive soil.
- It is shown that results got using the mathematical representation of the lightning current impulse with a Heidler function can be easily converted to other impulse representations, such as CIGRE and double-exponential functions.
- A general and straightforward method for evaluating optimal design enables the cost-effective analysis of the

counterpoise configurations as part of transmission line grounding for best protection against lightning effects.

II. Basic Assumptions

Despite the complexity of the physical processes of grounding systems dissipating the typical lightning current into the ground, simplifying assumptions is necessary to derive engineering formulas suitable for the early phases of grounding design. Such simplifications are also related to the "high degree of uncertainties involved in determining the relevant parameters and verification tests" [3]. It is, however, imperative that such assumptions must be conservative concerning safety.

A. Uniform Soil Model

This study considers the uniform soil model, characterized by constitutive parameters: resistivity, permittivity, and free space permeability. The apparent soil resistivity is determined from measurements [26], [27], while the relative permittivity is usually assumed, e.g., 10 to 15 (here we assumed value of 10). Although the two-layer soil model more accurately represents layered soil, the equivalent uniform model offers conservative results [28].

The non-linear behavior of ground resistivity with heavy currents due to soil ionization might improve the lightning performance of concentrated grounding systems [14]. However, this effect might be negligible on long counterpoises where the current dissipated per unit length is small [29]. Therefore, this effect is neglected in this study (see further discussion in Section XII). The second phenomenon that predicts improved lightning performance is the frequency dependence of the soil resistivity [12]. However, the knowledge of this complex phenomenon is incomplete [30], [31], [32], and analysis shows significant differences and inconsistencies "between the available models/expressions which are based on different sets of experimental data" [31]. Also, the impact of "the nonlinear variations of the soil moisture content" has to be further investigated [32]. Therefore, it is a conservative assumption to disregard this effect and assume constant soil resistivity.

B. Lightning Current Pulse Waveform

There is no consensus on the mathematical representation of current impulse waveforms of first and subsequent return strokes used in international standards and recommendations (see Fig. 1). IEEE standard [11] uses a double-exponential function. The second one is the current waveform recommended by the CIGRE study group [33], and the third is the analytical form of the current used in the International Electrotechnical Commission (IEC) standard [34] based on the Heidler function [35]. EPRI report [15] also used the latter. Fig. 1 illustrates the definitions of the front time T_1 for the different impulses used in [11], [33] and [34].

We use the Heidler function [35] from IEC standard [34] to represent the return-stroke current waveform (designated by IEC in Fig. 1):

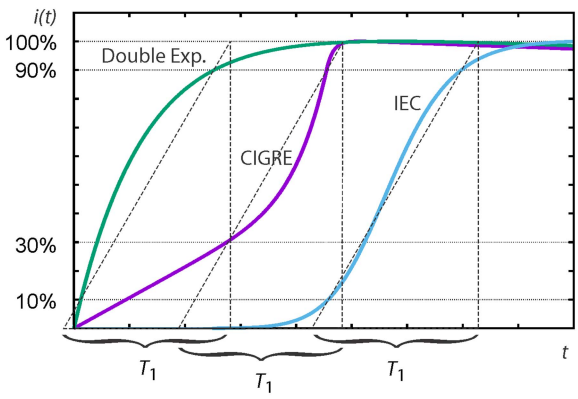

Fig. 1. The lightning current waveforms used in IEEE and IEC standards and CIGRE recommendations, and definitions of their front times T_1.

$$i(t) = \frac{1}{\eta} \cdot \frac{t^{10}}{t^{10} + \tau_1^{10}} \cdot e^{-t/\tau_2}. \tag{1}$$

The parameters η, τ_1, and τ_2 are determined for given values of the current peak, the front time T_1, and time-to-half-peak-value T_2 [35].

In Section XI, we show that, despite the considerable differences between the current impulses waveforms, the results got for the Heidler function (1) can be converted for the other two current waveforms in Fig. 1.

C. Quantities Used to Characterize Grounding's Lightning Performance

The low-frequency, low-current value of grounding resistance R is the primary quantity that characterizes grounding systems. The advantage of using R is that its value is easy to calculate or measure [27], [36]. R is linearly proportional to soil resistivity ρ, and R/ρ depends on the geometry of the grounding system.

R is also commonly used in lightning performance analysis, especially if the grounding system is smaller than the effective size. In such a case, the voltage $v(t)$ developed between the point where the lightning current $i(t)$ is injected into the grounding system and a distant neutral ground is

$$v(t) \approx Ri(t). \tag{2}$$

If the grounding system is larger than its effective size, then during the $i(t)$ initial rise and a period after the current peak I_m, $v(t)$ may be

$$v(t) > Ri(t). \tag{3}$$

In such a case, $v(t)$ may exhibit a significant peak V_m. The voltage and current peaks define the impulse impedance Z:

$$Z = \frac{V_m}{I_m}. \tag{4}$$

Z represents grounding systems in lightning performance analysis [37]. Z remains constant for all grounding system sizes larger than the effective one and $Z > R$. One goal of the grounding system design is to reduce the value of R by enlarging the

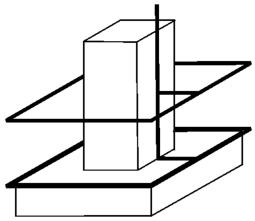

Fig. 2. A simple model of "double-loop" grounding connected to tower concrete foundations.

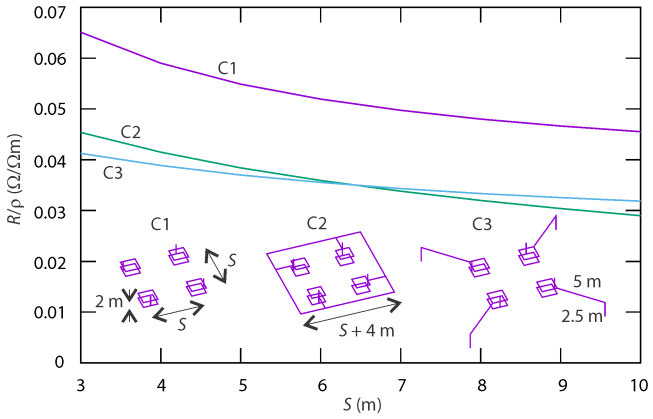

Fig. 3. Grounding resistivity R for any soil resistivity ρ of three TL concentrated grounding configurations.

grounding electrodes while keeping them smaller than their effective size for which $Z \approx R$.

III. Tower Footing Concentrated Grounds

Depending on the construction, the usual tower footing foundations include tower steel, grillage, and concrete/foundation reinforcing cages, which provide substantial grounding resistance [15]. Some constructions have two rings around the foundation (see Fig. 2). If the tower is accessible to the public, a potential control ring is often placed around the four footings (see configuration C2 in Fig. 3). If the required value of R is not achieved, radially connected ground rods are often installed. Such elements of the grounding system that are within about 15 meters of the tower base are known as "concentrated grounds" [2].

For example, Fig. 3 shows the range of R values for any ρ for the three grounding configurations (denoted as C1, C2, and C3) as a function of the footing distance. Additional electrodes in configurations C2 and C3 improve the grounding resistance in relation to C1, but further improvement is possible by connecting more extended electrodes. However, a suitable configuration of concentrated grounds usually can achieve a required value of R, e.g., $R \leq 10\,\Omega$, in soils with ρ smaller than about 300 Ωm.

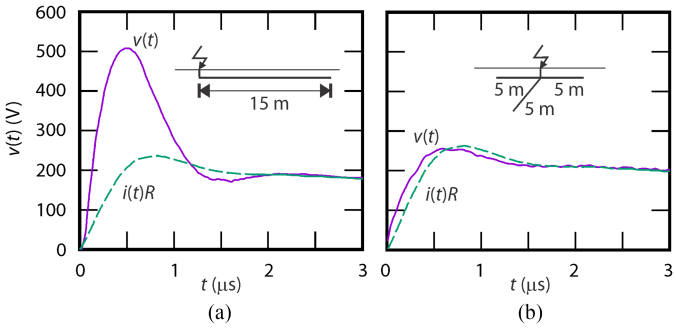

Fig. 4. (a) Measured current and voltage pulses in 15-m long buried wire. (b) Computed voltage for the same current pulse in wire divided into three 5-m long segments.

IV. Problem With Lightning Performance of Counterpoises and the Solution

Counterpoises are horizontal conductors buried in the earth at about 1 meter connected to the footings [2]. Counterpoises with extended lengths are often used to decrease tower grounding resistance in medium-to-high resistivity soils. However, Fig. 4(a) illustrates a problem with the lightning performance of counterpoises.

Fig. 4(a) shows recordings of one of the grounding system experiments for sub-microsecond rise time input current pulses that EdF conducted in Les Renardieres, France, from 1976 to 1978 [38], [25]. Fig. 4(a) shows measured voltage $v(t)$ at current injection point to neutral ground as a response to injected current pulse $i(t)$ with front time $T_1 \approx 0.47\,\mu s$ in 15-m long horizontal wire buried at 0.6 m in soil with $\rho = 79\,\Omega\mathrm{m}$ and $\varepsilon_\mathrm{r} = 15$ [1]. The performance during the current rise and short period after the current peak is much worse than during the rest of the impulse where $v(t) \approx Ri(t)$. In the initial period, due to the inductive behavior, $v(t)$ exhibits a peak of about 500 V, while the peak of $Ri(t)$ is near 200 V.

Bewley [39] has shown that such a performance can be improved if a single counterpoise is replaced with multiple shorter ones. This is illustrated in Fig. 4(b), where the 15-m wire is divided into three 5-m wires. Impulse performance is improved because of a much smaller inductive component of the three shorter wires than the single wire. The multiple wire resistivity is about 10% higher than the single wire because of mutual resistance between wire segments, but $v(t) \approx Ri(t)$ and $Z \approx R$, which is the desired design outcome.

The process of the counterpoise reconfiguration for better impulse performance in Fig. 4(a) and (b) can be viewed in terms of effective length. An effective area [40] can be imagined around the tower footings as circular areas with centers at the footings and radiuses equal to the effective length ℓ_{eff} (see Fig. 5). Multiple counterpoises connected radially to the footings, all within the effective area, reduce R while remaining $Z \approx R$. If the effective area goes beyond the right of way, the conductors can

[1] Interested reader can find details on the measuring setup and the influence of the measuring system on the results in [25].

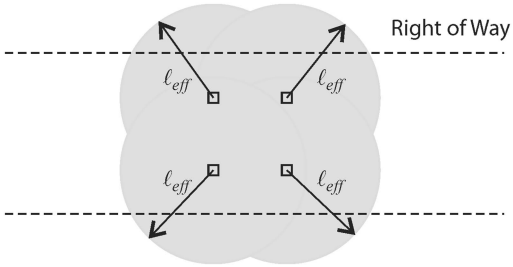

Fig. 5. Effective area around TL tower footings.

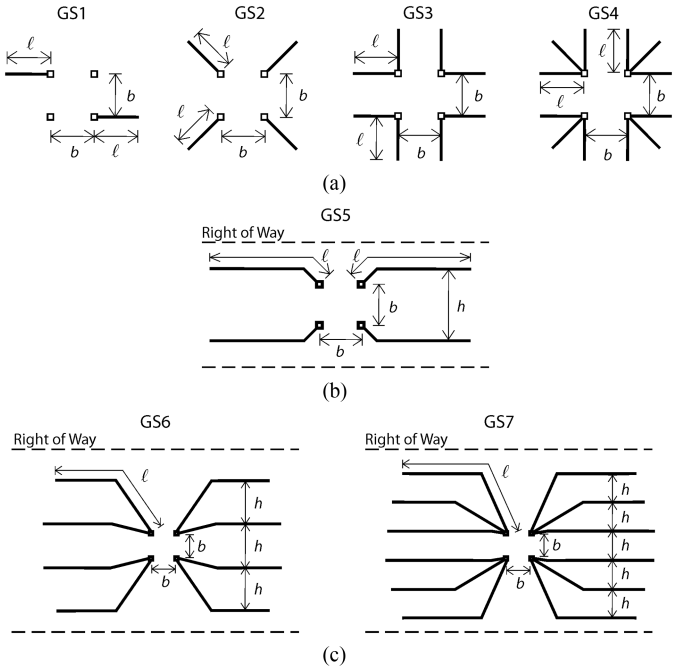

Fig. 6. (a) Counterpoises radially connected to TL tower footings. (b) Single counterpoises parallel to the line. (c) Multiple counterpoises parallel to the line.

be bent parallel to the line to stay within the right of way; it is crucial that they remain within the effective area.

V. Configurations of Counterpoises

Fig. 6 illustrates the configurations of counterpoises analyzed in this paper. 2-leg counterpoise, GS1 in Fig. 6(a), can be placed parallel to the line and the effective length limits its usability in more resistive soils. The others in Fig. 6(a), GS2, GS3, and GS4, are radial configurations recommended by France's EdF [41] and used in many countries [42]. However, they cover the entire effective area (see Fig. 5), which is limited by the right of way for practical reasons. Therefore, such practical considerations limit electrodes length that can be used to about 35 m [41], constraining their usability.

Configuration GS5 in Fig. 6(b) is one of the most often used. It is a variant of GS2 with bent counterpoises parallel to the line within the right-of-way. The effective length mainly limits its efficacy.

TABLE I
Values of the Geometric Parameters of Configurations in Fig. 6

		GS	Range (m)
Length	ℓ	all	1 – 100
Radius	a	all	0.007
Depth	d	all	0.5 – 1
Distance between footings	b	all	3 –10
Distance between parallel counterpoises	h	GS5	20 – 40
		GS6	10 – 20
		GS7	10 – 15

This paper proposes 8- and 12-leg configurations, GS6 and GS7 [see Fig. 6(c)], variants of GS3 and GS4, whose counterpoises are not radial but bent parallel to the line to remain within the right of way. Such a modification of the configurations allows for longer counterpoises and enlarges the total effective length. The distances between parallel counterpoises are 20 m or higher (for GS5) but can be 10 to 15 m (especially for GS7). All counterpoises in Fig. 6 have equal length ℓ and are connected to the current injection points, i.e., the tower's footings. The length ℓ is measured from the footing to the counterpoise open end. Ranges of the considered geometric parameters are given in Table I.

Comparison of the performances of these configurations is given in Section X.

VI. Approximation of Quantities That Characterize Lightning Performance

Grounding resistance *R* is expressed as a function of ℓ and impulse impedance *Z* is approximated by [40]:

$$Z = R(\ell),\ \ell \le \ell_{eff} \tag{5}$$

$$Z = R(\ell_{eff}),\ \ell > \ell_{eff} \tag{6}$$

Here, ℓ_{eff} is the effective length. Like ℓ, it is measured from the footing to the counterpoise open end. The definition of ℓ_{eff} is discussed in Section XIII.A.

ℓ_{eff} is approximated by an empirical formula [44]

$$\ell_{eff} = D\sqrt{\rho T_1} \tag{7}$$

where ρ is soil resistivity in Ωm, T_1 is lightning current pulse front time in μs. The constant *D* (7) is determined by the best fit of (6) to values of *Z* got by computer simulation with the rigorous electromagnetic model [18], [19], [20] (see Section VIII).

The interested readers can find more details on this method of approximating *Z* and ℓ_{eff} in [40].

VII. Low-Frequency Grounding Resistivity

Fig. 7 shows an example of the grounding resistance *R* of two configurations: C1, comprising four radial counterpoises alone, and C2, the counterpoises together with foundation grounding, as a function of the counterpoises length ℓ. It is shown that the influence of the local grounding system of the tower footings

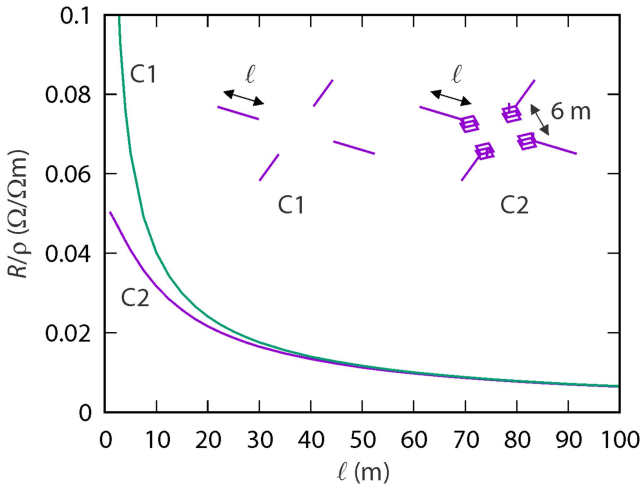

Fig. 7. Grounding resistance R for any soil resistivity ρ of four radial counterpoises alone (C1) and with footing groundings (C2).

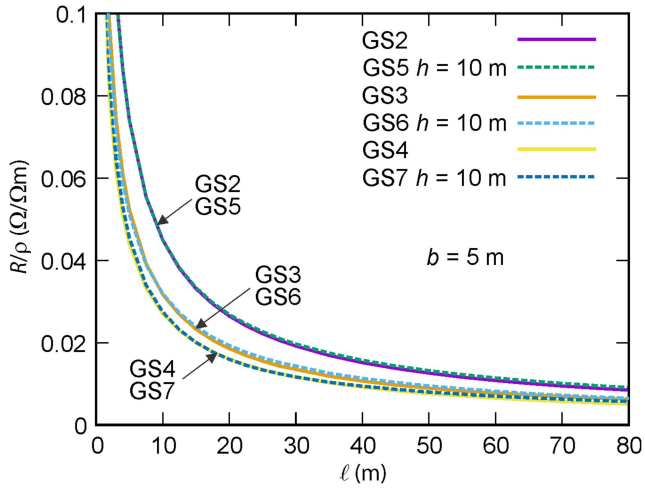

Fig. 9. Influence of h on R/ρ of configurations in Fig. 6 (simulation results).

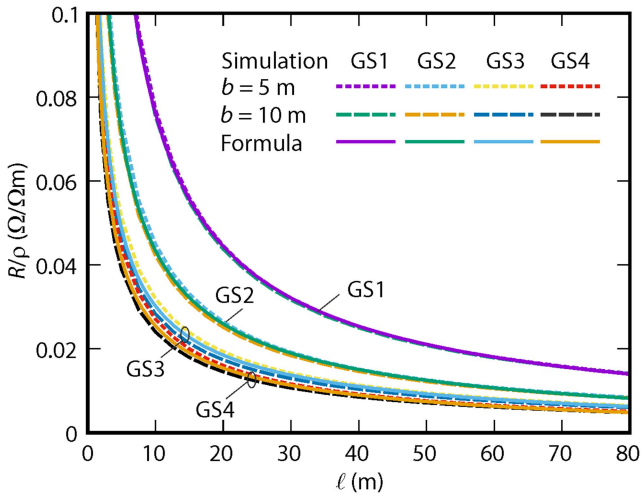

Fig. 8. Influence of b on R/ρ of configurations GS1, GS2, GS3, and GS4 in Fig. 6 [simulation results and formula (8)].

TABLE II
PARAMETER VALUES IN FORMULAS FOR RESISTIVITY (8) AND EFFECTIVE LENGTH (7) OF COUNTERPOISE CONFIGURATIONS IN FIG. 6

	A	B	C	D
GS1	–0.0032	0.432	–0.736	1.059
GS2	–0.0032	0.221	–0.676	1.127
GS3	–0.0021	0.144	–0.649	1.285
GS4	–0.0024	0.124	–0.648	1.310
GS5	–0.0023	0.221	–0.681	1.136
GS6	–0.0017	0.153	–0.678	1.226
GS7	–0.0013	0.130	–0.678	1.254

becomes negligible concerning the resistance of longer counterpoises. Therefore, analysis of long counterpoises alone will lead to results relevant to the complete tower grounding system.

It is well known that the burial depth and the radius of the counterpoises have a minor influence on R [26].

Fig. 8 shows that the distance between the tower's footings, b, influences the R values, especially for configurations with multiple counterpoises (GS3 and GS4). The differences of R are within 10%. Results in Fig. 8 are for the radial configurations, but the conclusions are similar for the others.

The simulation results of R in Fig. 9 show minor differences between radial and bent counterpoises parallel to the line when the distance between parallel counterpoises, h, is greater or equal to 10 m. The examples in Fig. 9 are for the distance between tower footings $b = 5$ m, but the conclusions are the same for other distances.

Therefore, it is possible to derive a single formula that approximates R of a particular configuration for all considered distances between footings and parallel counterpoises (see Table I):

$$R = \rho\left(A + B\ell^{C}\right) \tag{8}$$

where values of A, B, and C are given in Table II for all configurations in Fig. 6. Fig. 8 shows the simulation results and (8). The error of (8) considering simulation results is smaller than 10%.

Figs. 8 and 9 also show that 8-leg counterpoises, GS3, and GS6, significantly reduce R compared to 4-leg counterpoises, GS2 and GS5. The decrease is about 30% for any length ℓ. However, the reduction of R by 12-leg counterpoises, GS4 and GS7, in comparison to GS3 and GS6, is smaller, about 10%.

The following are more accurate formulas of R that, besides ρ and ℓ, consider values of conductor radius a, depth of burial d, and distance between tower footings b. The method for deriving the formulas is described in [40].

$$\text{GS1}: R = \frac{\rho}{4\pi\ell}\left[\ln\frac{2\ell}{a} + \ln\frac{2}{d} - 1.5428 + 0.1319\frac{b}{\ell} - 0.2779\ln\frac{b}{\ell}\right] \tag{9}$$

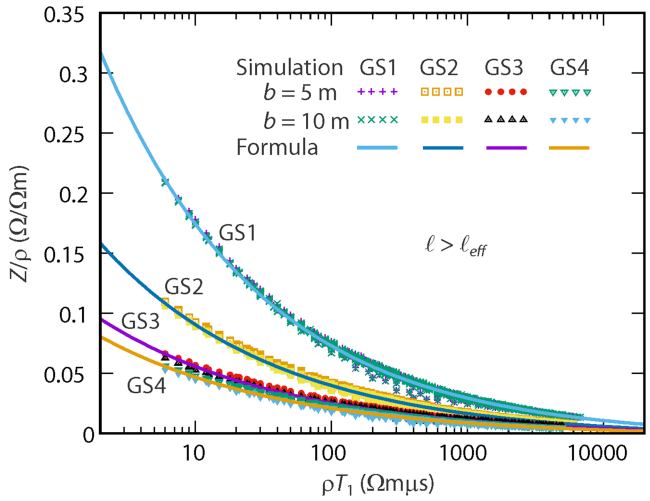

Fig. 10. Simulation results of Z and formula (16) that fits the simulation results for GS1, GS2, GS3, and GS4 configurations (see Fig. 6).

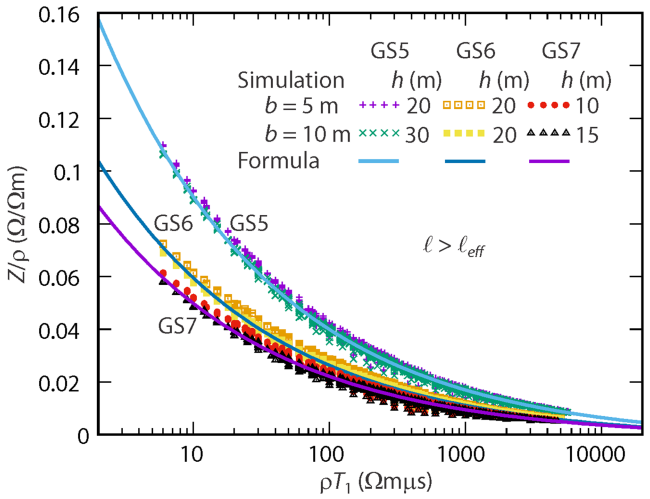

Fig. 11. Simulation results of Z and formula (16) that fits the simulation results for GS5, GS6, and GS7 configurations (see Fig. 6).

$$\text{GS2}: R=\frac{\rho}{8\pi\ell}\left[\ln\frac{2\ell}{a}+\ln\frac{\ell}{d}+0.2647-0.5965\frac{b}{\ell}-0.6719\ln\frac{b}{\ell}\right] \tag{10}$$

$$\text{GS3}: R=\frac{\rho}{16\pi\ell}\left[\ln\frac{2\ell}{a}+\ln\frac{\ell}{d}+3.1649+0.3036\frac{b}{\ell}-2.3945\ln\frac{b}{\ell}\right] \tag{11}$$

$$\text{GS4}: R=\frac{\rho}{24\pi\ell}\left[\ln\frac{2\ell}{a}+\ln\frac{\ell}{d}+6.6469+0.3767\frac{b}{\ell}-3.4\ln\frac{b}{\ell}\right] \tag{12}$$

$$\text{GS5}: R=\frac{\rho}{8\pi\ell}\left[\ln\frac{2\ell}{a}+\ln\frac{\ell}{d}-0.8054+0.4758\frac{b}{\ell}-1.3536\ln\frac{b}{\ell}\right] \tag{13}$$

$$\text{GS6}: R=\frac{\rho}{12.5\pi\ell}\left[\ln\frac{2\ell}{a}+\ln\frac{\ell}{d}+0.1619+0.243\frac{b}{\ell}-1.4939\ln\frac{b}{\ell}\right] \tag{14}$$

$$\text{GS7}: R=\frac{\rho}{19.9\pi\ell}\left[\ln\frac{2\ell}{a}+\ln\frac{\ell}{d}+2.0907+2.622\frac{b}{\ell}-3.7192\ln\frac{b}{\ell}\right] \tag{15}$$

VIII. Impulse Impedance and Effective Length

Applying (5), (6), and (8), Z is expressed as:

$$Z=\rho\left[A+B\left(D\sqrt{\rho T_1}\right)^C\right],\ \ell>\ell_{eff} \tag{16}$$

where values of A, B, C, and D are given in Table II. The constant D is determined by the best fit of (16) to simulation results of Z (see Figs. 10 and 11). The simulation results are derived from time responses of 11386 test cases for each configuration with parameters in wide ranges (ρ from 30 to 2000 Ωm, T_1 from 0.2 to 10 μs, and ℓ from 1 to 100 m). Figs. 10 and 11 illustrate a remarkable outcome that simulation results of Z/ρ as a function of ρT_1 converge to a generalized curve, enabling a single approximating function (16).

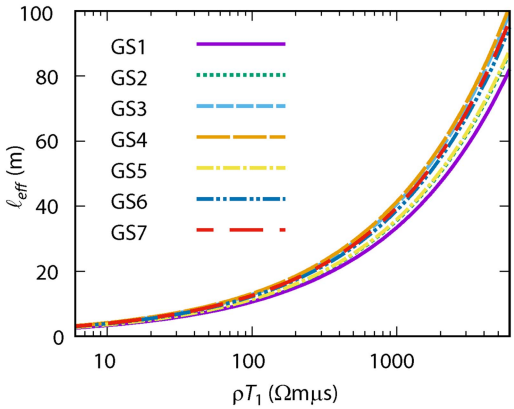

Fig. 12. Effective lengths of counterpoise configurations in Fig. 6.

Similar to the results for R in the previous section, Figs. 10 and 11 show that 8-leg counterpoises, GS3 and GS6, considerably reduce Z compared to 4-leg configurations, GS2 and GS5, but 12-leg counterpoises, GS4 and GS7, have a much smaller effect.

Figs. 10 and 11 show results of (16) that uses (8) to approximate Z. The error of the formula (16) considering the simulation results for GS5 in Fig. 11 is smaller than 5% in 97% of the test cases. Errors of other configurations are similar. However, more accurate (9)–(15) can be used instead of (8) to approximate Z considering conductor radius, a, distance between footings, b, and depth, d.

Fig. 12 shows the effective length of all counterpoise configurations in Fig. 6 for any values of ρ and T_1 computed by (7) with values of D in the last column of Table II. Configurations with multiple counterpoises have smaller inductive components and correspondingly larger ℓ_{eff} (and larger effective areas, see Fig. 5). Configurations with the same number of legs bent parallel to the line have smaller effective lengths than radial ones.

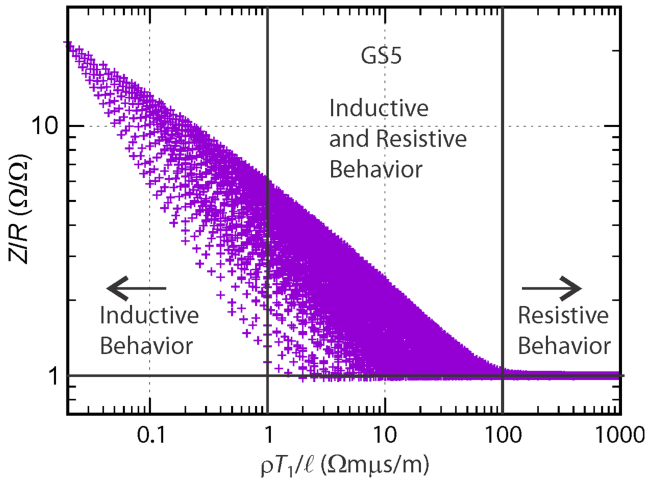

Fig. 13. Simulation results of Z/R for 11386 test cases with parameters in ranges (ℓ from 1 to 100 m; ρ from 30 to 2000 Ωm; T_1 from 0.2 to 10 μs) for configuration GS5.

IX. Ranges of Parameters for Conductive and Inductive Behavior

Fig. 13 shows all simulation results of *Z*/*R* that are derived from time responses of 11386 test cases for the configuration GS5 (see Fig. 6). Results for other configurations are similar. The results enable approximating ranges of parameters when grounding systems exhibit dominantly resistive ($Z/R \approx 1$) or inductive behavior ($Z/R > 1$):

$$\begin{aligned}
&\rho T_1/\ell < 1, \quad \text{inductive effects}\\
&\rho T_1/\ell > 100, \quad \text{resistive effects}\\
&1 < \rho T_1/\ell < 100 \quad \text{and} \quad \ell < \ell_{eff}, \quad \text{resistive effects}\\
&1 < \rho T_1/\ell < 100 \quad \text{and} \quad \ell > \ell_{eff}, \quad \text{inductive effects}
\end{aligned}$$

Visacro et al. [45] state that *Z*/*R* "is typically lower than 1 for electrode lengths shorter than ℓ_{eff}, due to the effects of capacitive currents in the soil." Our computations do not show any significant impact of the capacitive effect on the values of *Z*/*R*, as shown in Fig. 13. The dominantly capacitive effect is typical for less extended electrodes in high resistivity soil. For example, in our computations, the voltage impulse lags the current, and its front time becomes longer in the case of dominantly capacitive behavior. Still, the voltage peak value V_{m} is not significantly reduced, which results in $Z/R \approx 1$.

X. Comparison Between Configurations

The length of counterpoises ℓ for obtaining the required value of resistance *R* for a given resistivity of soil ρ can be determined from (8):

$$\ell = \left(\frac{R/\rho - A}{B}\right)^{\frac{1}{C}} \tag{17}$$

This formula is used for comparison between configurations. Fig. 14 shows counterpoises length ℓ necessary to get *R* values of 10 Ω, 15 Ω, and 20 Ω, as a function of the soil resistivity. Fig. 14 also shows the effective lengths ℓ_{eff} for values of T_1 of typical first and subsequent stroke, i.e., 2.4 μs and 0.35 μs [43]. To maintain $Z \approx R$, it is necessary that $\ell < \ell_{eff}$.

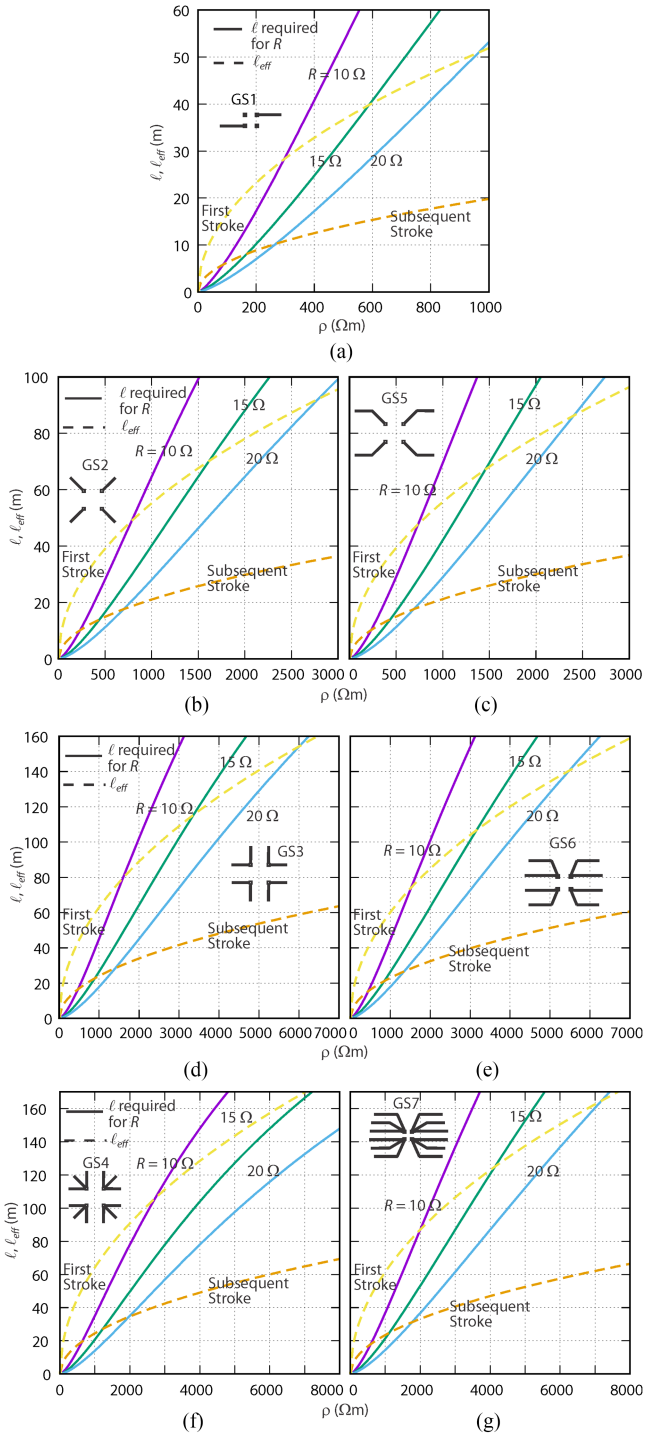

Fig. 14. Required counterpoises lengths to get resistivity of 10 Ω, 15 Ω, and 20 Ω, and the effective lengths for typical first and subsequent strokes for configurations: (a) GS1, (b) GS2, (c) GS5, (d) GS3, (e) GS6, (f) GS4, (g) GS7 (see Fig. 6).

Fig. 14 illustrates the capabilities and limitations of the considered configurations. The following conclusions can be drawn.

- The length ℓ of the radial counterpoises, GS2 in Fig. 14(b), GS3 in Fig. 14(d), and GS4 in Fig. 14(f), is limited to

TABLE III
RANGES OF SOIL RESISTIVITY AND THE REQUIRED LENGTHS OF COUNTERPOISE CONFIGURATIONS FOR $R \leq 10\,\Omega$

	ρ (Ωm)	ℓ (m)	$\ell_{(tot)}$(m)
GS1	up to 300	30	60
GS2	300–500	16–28	64–112
GS3	500–750	20–30	160–240
GS4	750–1000	26–35	312–420
GS5	up to 750	50	200
GS6	up to 1600	75	600
GS7	up to 2100	95	1140

about 35 m [41], which constrains their use. The other configurations within the right of way may use longer counterpoises, which may be limited by their effective lengths.

- More legs in 2-, 4-, 8-, and 12-leg counterpoises, GS1 in Fig. 14(a), GS2 (b) and GS5 (c), GS3 (d) and GS6 (e), and GS4 (f), extend their use in higher resistive soils. However, 12-leg counterpoise, GS7 in (g), is less effective.
- The efficiency of counterpoises bent parallel to the line (GS5 and GS6) whose distance between the parallel counterpoises is equal to or larger than 20 m is like the efficiency of radial ones (GS2 and GS3). Distances between counterpoises of GS7 are smaller, i.e., 10 and 15 m, and GS7 is considerably less efficient.
- The area covered by the considered configurations does not significantly impact the grounding system efficiency. That can be seen by comparison of the radial and bent configurations with the same number of legs, which cover different areas, i.e., 4-legs in Fig. 14(b) and (c), 8-legs in (d) and (e), and 12-legs in (f) and (g). The conductor length has the dominant impact on the efficiency.

Table III shows another example of the simple formulas use for comparison of the capabilities and limitations of the configurations. Table III gives lengths of counterpoise configuration in soil with different resistivity that are necessary to achieve R values of about 10 Ω. Values for GS2, GS3, and GS4 in Table III are adapted from EdF recommendations [41]. Connecting more counterpoises to the tower footing enables a larger conductor total length, resulting in lower R values in more resistive soils. The example in Table III shows that GS6 and GS7 enable $R \leq 10\,\Omega$ in soils with 1600 Ωm and 2100 Ωm.

XI. INFLUENCE OF CURRENT WAVEFORM

Fig. 15 shows simulation results of Z derived from time responses to two different mathematical representations of current waveforms of return strokes, i.e., used in IEC standards [34] and recommended by CIGRE [33] (see Section II.B). It is shown that results can be easily converted by modifying the impulse front time T_1:

$$T_{1(30-90\%)}^{(\mathrm{CIGRE})} = 1.82 \cdot T_{1(10-90\%)}^{(\mathrm{IEC})} \tag{18}$$

Note that definitions of the impulse front times are according to Fig. 1.

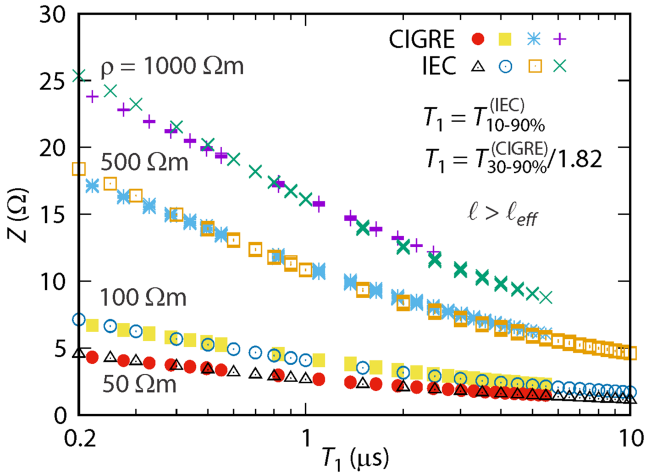

Fig. 15. Conversion of the simulation results of Z computed with IEC [34] and CIGRE [33] mathematical representations of current waveforms of the first return stroke (see Fig. 1). Simulations results are for GS5 configuration with $b = 6$ m and $h = 20$ m.

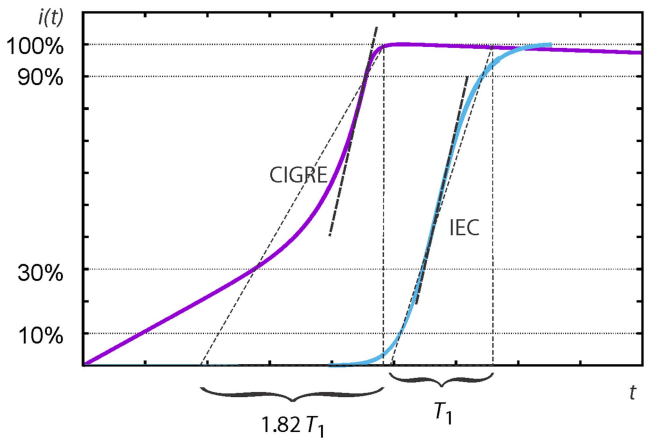

Fig. 16. The maximal steepness of the waveforms is similar when the CIGRE and IEC current waveforms are adjusted to lead to nearly identical Z.

Fig. 16 shows that when the CIGRE and IEC current waveforms are adjusted to lead to nearly identical results of Z, the maximal steepness of the waveforms is similar. This implies that the maximal steepness of these two current waveforms is one of the dominant factors that determines Z.

Fig. 17 shows that the double exponential mathematical representation of the current waveform leads to very similar results as the IEC waveform, and no adjustments are necessary.

XII. DISTRIBUTION OF LIGHTNING CURRENT BETWEEN LOCAL GROUNDING AND COUNTERPOISES

Fig. 18 shows an example of lightning current distribution between the local grounding and counterpoises for typical first and subsequent return stroke current impulses. The considered grounding system is configuration GS5 (see Fig. 6) with parameters shown in Fig. 18. The current dissipated through the local grounding and counterpoises is insufficient to have a significant soil ionization effect.

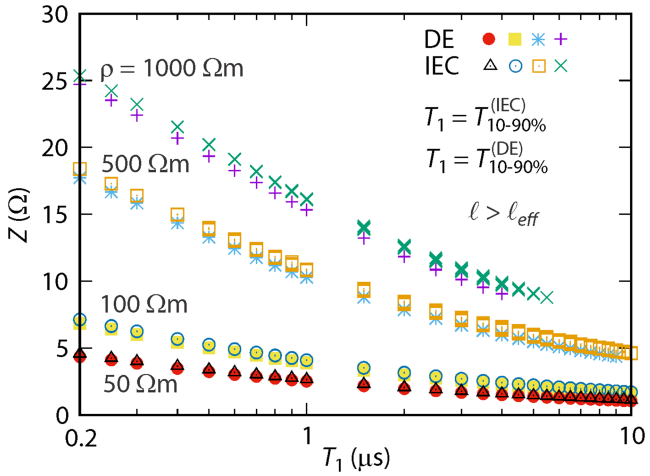

Fig. 17. The double exponential mathematical representation of the current waveform leads to very similar results as the IEC waveform.

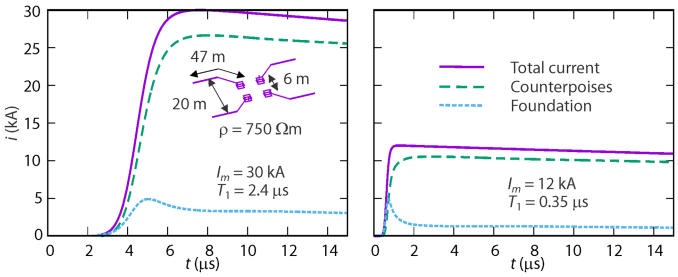

Fig. 18. The lightning current distribution between the local grounding and counterpoises for typical first and subsequent stroke current impulse.

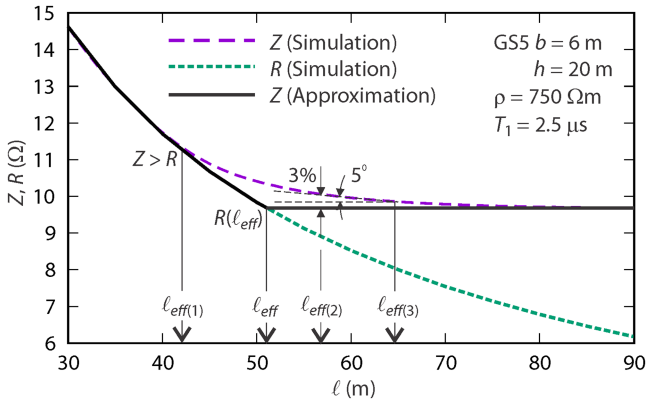

Fig. 19. Simulation results of R and Z (broken lines); approximation of Z [20] (full line); and different quantitative definitions of the effective length in literature: $\ell_{eff(1)}$ [43], ℓ_{eff} [40], $\ell_{eff(2)}$ [29], [44], $\ell_{eff(3)}$ [9].

XIII. Comparison With Previous Work

A. Effective Length

Effective length is defined concerning the change of Z when the length of electrodes enlarges. However, there are different definitions of effective length in the literature. Fig. 19 illustrates such definitions on an example of the grounding system GS5 [see Fig. 6(b)].

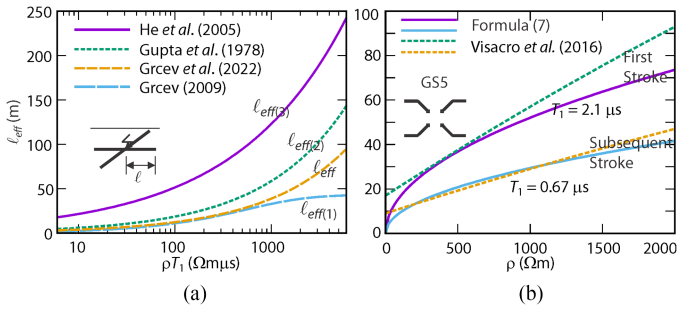

Fig. 20. (a) Comparison of effective length computed by formulas based on different definitions (labels are defined in Fig. 19). (b) Comparison between (7) and formulas in [45].

Simulation results in Fig. 19 show that $Z \approx R$ for counterpoise lengths smaller than a length denoted by $\ell_{eff(1)}$. Z becomes larger than R for counterpoise lengths larger than $\ell_{eff(1)}$, and, at more extensive lengths, converges to a constant value while R continuously decreases. Following quantitative definitions of effective length exist in the literature.

1) Gupta and Thapar [44], [29]: The length of an electrode when Z decreases to a value within 3% of the final value (denoted as $\ell_{eff(2)}$ in Fig. 19).
2) He et al. [9]: The length of a grounding electrode at which the derivative of Z with respect to ℓ is smaller than 5^0 (denoted as $\ell_{eff(3)}$ in Fig. 19).
3) Grcev [43]: Maximal length of the ground electrode for which $Z \approx R$, and above which $Z > R$ (denoted as $\ell_{eff(1)}$ in Fig. 19).
4) Grcev et al. [40]: The length for which R is equal to the Z final value (denoted as ℓ_{eff} in Fig. 19).

This paper uses the latter definition, denoted as ℓ_{eff} in Fig. 19. It enables the approximation of Z in (5) and (6) (represented by a full line in Fig. 19). (5) and (6) show that such an approximation leads to an outcome that only two quantities, i.e., resistivity R expressed as a function of ℓ, and effective length, ℓ_{eff}, are required to define the lightning performance of considered grounding systems.

Fig. 20(a) shows that the different definitions of the effective length lead to different results (the example is for the four-arm star configuration, shown in Fig. 20(a), for which corresponding formulas exist in the literature).

Fig. 20(b) shows a comparison of (7) with a formula published in [45]. The formulas in [45] differ significantly from this paper. They are specialized for one counterpoise configuration, i.e., GS5, and for two waveforms of the lightning current impulse, one for the first return stroke and the other for the subsequent stroke. The first one is a waveform with two peaks with $T_{30\text{-}90\%} = 3.83$ microseconds, represented by seven Heidler functions. The second is represented by two Heidler functions with $T_{30\text{-}90\%} = 0.67$ microseconds. In Fig. 20(b), T_1 for the first stroke is adapted to 3.83/1.82 =

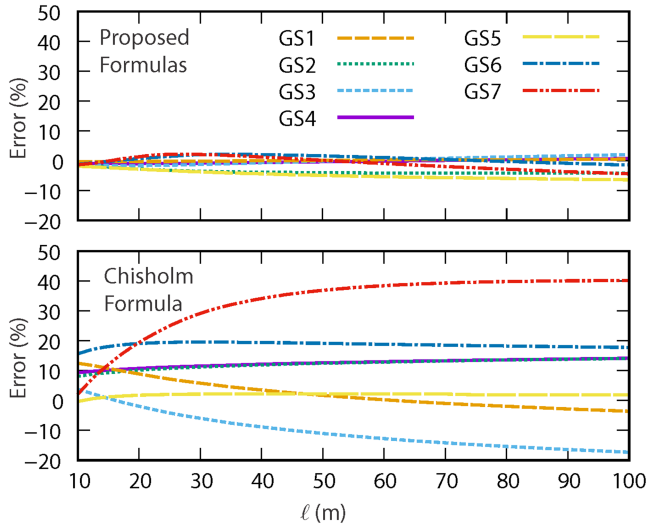

Fig. 21. Errors of formulas (9)–(15) and Chisholm formula [46] for each considered counterpoise configuration (see Fig. 6).

2.1 microseconds (since the two-peak waveform has a similar front to the CIGRE model). Results are similar for the subsequent stroke but diverge for the first stroke in high resistivity soil.

B. Low-Frequency Resistance

Chisholm's formula of R [46] is applicable for any grounding system form, from single rods to grids. Fig. 21 shows errors in this general formula and formulas (9)–(15). The reference values for evaluation errors are simulations by an accurate computer model [47]. The error of formulas (9)–(15) is less than 6%, while Chisholm [46] goes up to 40%.

XIV. Numerical Example

In this example, we look at the choice of the counterpoise configuration with $R = 10\ \Omega$ in the soil with $\rho = 1000\ \Omega$m, which requires the smallest total conductor length and develops a minimal voltage peak. The typical lightning first return stroke's current peak and front time are $I_{\rm m} = 30$ kA and $T_1 = 2.4\ \mu s$, and of the subsequent return stroke $I_{\rm m} = 12$ kA and $T_1 = 0.35\ \mu s$ [43].

The results of computations by the developed formulas are in Table IV. The following steps lead to these results.

Columns 1 and 2: For each configuration, length ℓ and total conductor length ℓ_{tot} are computed by (17) using values of A, B, and C in Table II and $\ell_{tot} = n\ell$, where n is the number of legs in the configuration.

Columns 3 and 4: Effective lengths for the first and subsequent return strokes, ℓ_{effFS} and ℓ_{effSS}, are computed by (7) using values of D from Table II.

Columns 5 and 6: Impulse impedances for the first and subsequent return strokes, $Z_{\rm FS}$ and $Z_{\rm SS}$, are computed by (16) using values of A, B, C, and D from Table II. More accurate values can be computed by (9)–(15) with $\ell = \ell_{effFS}$ and ℓ_{effSS} computed by (7) and values of D from Table II.

TABLE IV
Computation Results ($\rho = 1000\Omega$m and $R = 10\Omega$)

GS	1 ℓ (m)	2 $\ell_{\rm tot}$ (m)	3 ℓ_{effFS} (m)	4 ℓ_{effSS} (m)	5 $Z_{\rm FS}$ (Ω)	6 $Z_{\rm SS}$ (Ω)	7 $V_{m\rm FS}$ (kV)	8 $V_{m\rm SS}$ (kV)
GS1	114	228	52	20	21	44	630	528
GS2	65	260	55	21	12	25	360	300
GS3	45	360	63	24	10	16	300	192
GS4	35	420	64	25	10	13	300	156
GS5	70	280	56	21	12	25	360	300
GS6	44	352	60	23	10	17	300	204
GS7	37	444	61	23	10	14	300	168

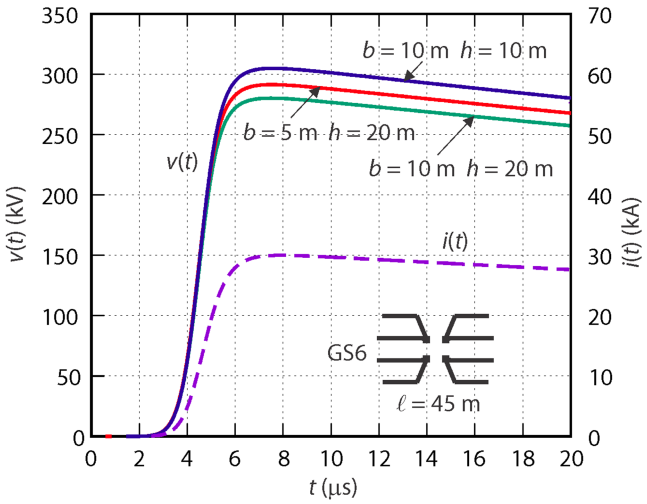

Fig. 22. Voltages developed at the counterpoise configuration GS6 in case of typical first stroke lightning current impulse.

Columns 7 and 8: Voltage peaks for the first and subsequent return strokes, $V_{m\rm FS}$ and $V_{m\rm SS}$, are computed by (4).

8-leg counterpoise GS6 might be chosen for the optimal configuration with $\ell = 44$ m since the total length of 352 m is the smallest and $V_{m\rm FS} = 300$ kV is minimal while $V_{mSS} < V_{m\rm FS}$. Note that EdF recommends using GS4 in this case [41], but it requires a total conductor length of 420 m.

Since the formulas are approximate, we check the correctness of this solution by computing the developed voltage in the case of the first return stroke with the rigorous electromagnetic model [20]. Fig. 22 shows the simulation results. The distance between the tower footings, b, is 5 or 10 m, and between the parallel counterpoises, h, is 10 or 20 m. Although there are differences of about 10%, it can be seen that voltages in all cases are consistent with the requirement of $V_{m\rm FS} = 300$ kV.

Note that the numerical example results in this Section depend on input data and do not imply that GS6 is optimal in all cases. The trends can be studied in Fig. 14. A comparison can be made by generating results such as in Table IV for given values of R, ρ, and $I_{\rm m}$ and T_1 of the first and subsequent return stroke current (represented by CIGRE, IEC or double-exponential waveforms).

XV. Conclusion

1) Radial 4-, 8- and 12-leg counterpoises are limited to about 35 m because of practical considerations. 2- and 4-leg counterpoises bent parallel to the line have no such limitation, but their effective length constrains the use in high resistivity soil.
2) This paper proposes an 8-leg counterpoise bent parallel to the line. This counterpoise enlarges the effective length and is efficient in high resistive soil. A 12-leg counterpoise bent parallel to the line is less effective.
3) The influence of the mutual resistances between the parallel counterpoises is negligible for 20 m or higher distances. Counterpoises as close as 10 m can also be used, leading to about 10% higher peak voltages.
4) A complete set of new simple formulas of resistance, impulse impedance, and effective length of all considered counterpoise configurations is derived.
5) Remarkably, simulation results of Z/ρ as a function of ρT_1 converge to a generalized curve, enabling a single approximating function.
6) Ranges of parameters for which behavior is dominantly resistive or inductive are determined.
7) It is shown that impulse impedance results got for the different mathematical representations of the lightning current impulses such as Heidler, CIGRE, and double-exponential functions, can be easily mutually converted.
8) Different definitions of the effective length in the literature lead to different results. The definition used in this paper is consistent with a large number of simulation results.
9) New formulas and procedures make up a general and straightforward method for analyzing the optimal design of counterpoises as part of transmission line grounding, considering the cost-effective and best protection against lightning.
10) The underlying simplifications of the formulas are conservative and can be used in the initial grounding design phase. If more detailed data on soil characteristics from measurements on the actual site is available, more elaborate models and dedicated software, e.g., [48], might allow for more accurate computations.

References

[1] W. W. Lewis, *The Protection of Transmission Systems Against Lightning*. New York, NY, USA: Dover, 1965.
[2] A. R. Hileman, *Insulation Coordination for Power Systems*. Boca Raton, FL, USA: CRC, 1999.
[3] F. Kiessling, P. Nefzger, J. F. Nolasco, and U. Kaintzyk, *Overhead Power Lines*. Berlin, Germany: Springer, 2003.
[4] Y. Liu, N. Theethayi, and R. Thottappillil, "Investigating the validity of existing definitions and empirical equations of effective length/area of grounding wire/grid for transient studies," *J. Electrostatics*, vol. 65, no. 5/6, pp. 329–335, May 2007.
[5] S. Miyamoto et al., "Effective length of vertical grounding wires connected to wind turbine foundation," *J. Int. Council Elect. Eng.*, vol. 7, no. 1, pp. 89–95, May 2017.
[6] K. Yamamoto, S. Sumi, S. Sekioka, and J. He, "Derivations of effective length formula of vertical grounding rods and horizontal grounding electrodes based on physical phenomena of lightning surge propagations," *IEEE Trans. Ind. Appl.*, vol. 51, no. 6, pp. 4034–4042, Nov./Dec. 2015.
[7] O. Kherif, S. Chiheb, M. Teguar, A. Mekhaldi, and N. Harid, "Investigation of horizontal ground electrode's effective length under impulse current," *IEEE Trans. Electromagn. Compat.*, vol. 61, no. 5, pp. 1515–1523, Oct. 2019.
[8] S. Sekioka and T. Funabashi, "A study on effective length for practical design of grounding system in a wind turbine," in *Proc. Int. Conf. Lightning Protection*, Cagliari, Italy, 2010, pp. 1–6.
[9] J. He et al., "Effective length of counterpoise wire under lightning current," *IEEE Trans. Power Del.*, vol. 20, no. 2, pp. 1585–1591, Apr. 2005.
[10] J. He, R. Zeng, and B. Zhang, *Methodology and Technology for Power System Grounding*. New York, NY, USA: Wiley, 2013.
[11] *IEEE Guide for Improving the Lightning Performance of Transmission Lines*, IEEE Standard 1243-1997, Dec. 1997.
[12] W. Chisholm et al., "Impact of soil-parameter frequency dependence on the response of grounding electrodes and on the lightning performance of electrical systems," CIGRE, Paris, France, Tech. Brochure 781, 2019.
[13] CIGRE, "Procedures for estimating the lightning performance of transmission lines – new aspects," CIGRE, Paris, France, Tech. Brochure 839, 2021.
[14] "Tower grounding and soil ionization report," EPRI, Palo Alto, CA, Tech. Rep. 1001908, 2002.
[15] "Handbook for improving overhead transmission line lightning performance," EPRI, Palo Alto, CA, USA, Rep. 1002019., 2002.
[16] "Guide for transmission line grounding: A roadmap for design, testing, and remediation: Part I—Theory book," EPRI, Palo Alto, CA, USA, Tech. Rep. 1013900., 2007.
[17] P. Chowdhuri, *Electromagnetic Transients in Power Systems*. Hoboken, NJ, USA: Wiley, 1996.
[18] L. Grcev and Z. Haznadar, "A novel technique of numerical modelling of impulse current distribution in grounding systems," in *Proc. Int. Conf. Lightning Protection*, Graz, Austria, 1988, pp. 165–169.
[19] L. Grcev and F. Dawalibi, "An electromagnetic model for transients in grounding systems," *IEEE Trans. Power Del.*, vol. 5, no. 4, pp. 1773–1781, Oct. 1990.
[20] B. Markovski, L. Grcev, and V. Arnautovski-Toseva, "Fast and accurate transient analysis of large grounding systems in multilayer soil," *IEEE Trans. Power Del.*, vol. 36, no. 2, pp. 598–606, Apr. 2021.
[21] R. G. Olsen and M. C. Willis, "A comparison of exact and quasi-static methods for evaluating grounding systems at high frequencies," *IEEE Trans. Power Del.*, vol. 11, no. 3, pp. 1071–1081, Apr. 1996.
[22] L. Grcev and V. Arnautovski, "Comparison between simulation and measurement of frequency dependent and transient characteristics of power transmission line grounding," in *Proc. Int. Conf. Lightning Protection*, Birmingham, U.K., 1998, vol. 1, pp. 524–529.
[23] L. Grcev, "Computer analysis of transient voltages in large grounding systems," *IEEE Trans. Power Del.*, vol. 11, no. 2, pp. 815–823, Apr. 1996.
[24] L. Grcev, "Time- and frequency-dependent lightning surge characteristics of grounding electrodes," *IEEE Trans. Power Del.*, vol. 24, no. 4, pp. 2186–2196, Oct. 2009.
[25] R. G. Olsen and L. Grcev, "Analysis of high-frequency grounds: Comparison of theory and experiment," *IEEE Trans. Ind. Appl.*, vol. 51, no. 6, pp. 4889–4899, Nov./Dec. 2015.
[26] G. F. Tagg, *Earth Resistances*. London, U.K.: Newnes, 1964.
[27] *IEEE Guide for Measuring Earth Resistivity, Ground Impedance, and Earth Surface Potentials of a Grounding System*, IEEE Standard 81, IEEE, Manhattan, NY, USA, 2012.
[28] P. Dawalibi and R. D. Southey, "On the equivalence of uniform and two-layer soils to multilayer soils in the analysis of grounding systems," *IEE Proc. Gener. Transmiss. Distrib.*, vol. 143, no. 1, pp. 49–55, Jan. 1996.
[29] B. R. Gupta and B. Thapar, "Impulse impedance of grounding grids," *IEEE Trans. Power App. Syst.*, vol. PAS-99, no. 6, pp. 2357–2362, Nov. 1980.
[30] L. Grcev, "High-frequency grounding," in *Lightning Protection*, V. Cooray, Ed., London, U.K.: The Inst. Eng. Technol., 2009, pp. 503–527.
[31] D. Cavka, N. Mora, and F. Rachidi, "A comparison of frequency-dependent soil models: Application to the analysis of grounding systems," *IEEE Trans. Electromagn. Compat.*, vol. 56, no. 1, pp. 177–187, Feb. 2014.
[32] M. Nazari, R. Moini, S. Fortin, F. P. Dawalibi, and F. Rachidi, "Impact of frequency-dependent soil models on grounding system performance for direct and indirect lightning strikes," *IEEE Trans. Electromagn. Compat.*, vol. 63, no. 1, pp. 134–144, Feb. 2021.
[33] *Guide to Procedures for Estimating the Lightning Performance of Transmission Lines, Working Group 01 (Lightning) of Study Committee 33*, CIGRE, Paris, France, Tech. Brochures 63, 1991.
[34] *Protection Against Lightning - Part 1: General Principles*, International Electrotechnical Commission IEC 62305-1, Geneva, Switzerland, Int. Std. IEC 62305-1, Dec. 2010.

[35] F. Heidler, J. M. Cvetic, and B. V. Stanic, "Calculation of lightning current parameters," *IEEE Trans. Power Del.*, vol. 14, no. 2, pp. 399–404, Apr. 1999.
[36] *IEEE Guide for Safety in AC Substation Grounding*, IEEE Std. 80-2013, IEEE, Manhattan, NY, USA, Dec. 2013.
[37] S. Visacro, "The use of the impulse impedance as a concise representation of grounding electrodes in lightning protection applications," *IEEE Trans. Electromagn. Compat.*, vol. 60, no. 5, pp. 1602–1605, Oct. 2018.
[38] R. Fieux, P. Kouteynikoff, and F. Villefranque, "Measurement of the impulse response of groundings to lightning currents," in *Proc. Int. Conf. Lightning Protection*, Paper 4.3, pp. K4:40–K4:55, Uppsala, Sweden, 1979.
[39] L. V. Bewley, *Traveling Waves on Transmission Lines*. New York, NY, USA: Wiley, 1951.
[40] L. Grcev, B. Markovski, and M. Todorovski, "Lightning performance of multiple horizontal, vertical and inclined grounding electrodes," *IEEE Trans. Power Del.*, early access, Dec. 21, 2021, doi: 10.1109/TPWRD.2021.3137361.
[41] *Guide D'application De La Note H115 – Principes de Mise à La Terre Des Ouvrages Du Service du Transport et Des Télécommunications*, Paris, France: Électricité de, Sep. 1991.
[42] F. M. Gatta, A. Geri, S. Lauria, and M. Maccioni, "Simplified HV tower grounding system model for backflashover simulation," *Elect. Power Syst. Res.*, vol. 85, pp. 16–23, Apr. 2012.
[43] L. Grcev, "Impulse efficiency of ground electrodes," *IEEE Trans. Power Del.*, vol. 24, no. 1, pp. 441–451, Jan. 2009.
[44] B. R. Gupta and B. Thapar, "Impulse impedance of grounding systems," *IEEE Trans. Power App. Syst.*, vol. PAS-99, no. 6, pp. 2357–2362, Nov. 1980.
[45] S. Visacro and F. H. Silveira, "Lightning performance of transmission lines: Requirements of tower-footing electrodes consisting of long counterpoise wires," *IEEE Trans. Power Del.*, vol. 31, no. 4, pp. 1524–1532, Aug. 2016.
[46] W. A. Chisholm, "Evaluation of simple models for the resistance of solid and wire-frame electrodes," *IEEE Trans. Ind. Appl.*, vol. 51, no. 6, pp. 5123–5129, Nov./Dec. 2015.
[47] R. P. Nagar, R. Velazquez, M. Loeloeian, D. Mukhedkar, and Y. Gervdis, "Review of analytical methods for calculating the performance of large grounding electrodes part 1: Theoretical considerations," *IEEE Trans. Power App. Syst.*, vol. PAS-104, no. 11, pp. 3123–3133, Nov. 1985.
[48] "TRAGSYS-software for high frequency and transient analysis of grounding systems," version. 2.0 2005. [Online]. Available: http://www.tragsys.com

IEEE TRANSACTIONS ON
POWER DELIVERY

IEEE POWER & ENERGY SOCIETY

APRIL 2023 VOLUME 38 NUMBER 2 ITPDE5 (ISSN 0885-8977)

(Contents Continued on Page 753)

(Contents Continued from Front Cover)

(Contents Continued on Page 754)

(Contents Continued from Page 753)

POWER & ENGINEERING LETTER

IEEE POWER & ENERGY SOCIETY

The IEEE Power & Energy Society is an organization of IEEE members whose principal interest is in the advancement of the science and practice of electric power generation, transmission, distribution, and utilization. For membership and subscription information and pricing, please visit www.ieee.org/membership-catalog.

IEEE Transactions on Power Delivery (ISSN 0885-8977) is published bimonthly by The Institute of Electrical and Electronics Engineers, Inc. Responsibility for the contents rests upon the authors and not upon the IEEE, the Society, or its members. **IEEE Corporate Office:** 3 Park Avenue, 17th Floor, New York, NY 10016. **IEEE Operations Center:** 445 Hoes Lane, Piscataway, NJ 08854. **NJ Telephone:** +1 732 981 0060. **Price/Publication Information:** Individual copies: To order individual copies for members and nonmembers, please email the IEEE Contact Center at contactcenter@ieee.org. (Note: Postage and handling charge not included.) Member and nonmember subscription prices available upon request. **Copyright and Reprint Permissions:** Abstracting is permitted with credit to the source. Libraries are permitted to photocopy for private use of patrons, provided the per-copy fee of $31.00 is paid through the Copyright Clearance Center, 222 Rosewood Drive, Danvers, MA 01923. For all other copying, reprint, or republication permission, write to: Copyrights and Permissions Department, IEEE Publications Administration, 445 Hoes Lane, Piscataway, NJ 08854.

Periodicals Postage Paid at New York, NY and at additional mailing offices. **Postmaster:** Send address changes to IEEE Transactions on Power Delivery, IEEE, 445 Hoes Lane, Piscataway, NJ 08854. GST Registration No. 125634188. CPC Sales Agreement #40013087. Return undeliverable Canada addresses to: Pitney Bowes IMEX, P.O. Box 4332, Stanton Rd., Toronto, ON M5W 3J4, Canada. IEEE prohibits discrimination, harassment and bullying. For more information, visit http://www.ieee.org/nondiscrimination. Printed in USA.

Digital Object Identifier 10.1109/TPWRD.2023.3253240